Significance of Rotating Ground Motions on Behavior of Symmetric- and Asymmetric-plan Structures: Part 2. Case Studies

Erol Kalkan, [a] **M.EERI and Juan C. Reyes,** [b]

The influence of the ground motion rotation angle on several engineering demand parameters (EDPs) is systematically examined by a parametric study in the companion paper based on three-dimensional (3D) computer models of single-story systems by varying their vibration period and response modification factor *R*. Further validations are performed here using 3D computer models of 9-story buildings that have symmetric and asymmetric layouts subjected to a suite of bi-directional near-fault records with and without distinct velocity-pulses. The exhaustive set of linear and nonlinear response history analyses (RHAs) are used for evaluating the use of the fault-normal and fault-parallel (FN/FP) directions and maximum-direction (MD) to rotate ground motions. The findings of this study suggest that ground motions rotated to FN/FP direction or MD do not necessarily provide conservative values of EDPs in nonlinear-inelastic range, but rather, they tend to produce larger EDPs than as-recorded (arbitrarily oriented) motions from RHAs.

INTRODUCTION

When response history analysis (RHA) is required for design verification of building structures, the International Building Code (ICBO, 2009) and California Building Code (ICBO, 2010) refer to the ASCE/SEI-7 Section 16.2 (ASCE, 2006, 2010). According to these standards, at least two horizontal ground motion components should be considered for 3D RHA of structures. At sites within 5 km of the active fault that dominates the hazard, each pair of ground motion components should be rotated to the fault-normal and fault-parallel (FN/FP) directions. In addition, ASCE/SEI 7-10 (Chapter 21) defines maximum-direction (MD) ground motion, a revised definition of horizontal ground motions to develop site-specific design spectrum as an alternative to code-based design spectrum per ASCE/SEI 7-10

[a] United States Geological Survey, Menlo Park, California; *ekalkan@usgs.gov* (corresponding author)
[b] Universidad de los Andes, Bogota, Colombia; *jureyes@uniandes.edu.co*

(Chapter 11) based on mapped spectral acceleration values at short period (S_S) and at 1 second period (S_1). Note that the MD is the direction associated with the peak response of a two-degrees-of-freedom system with equal stiffness and damping ratio in the *x* and *y* axes subjected to bi-directional excitation (Huang et al., 2008).

In the companion paper (Reyes and Kalkan, 2012a), the influence of rotation angle of the ground motion on several engineering demand parameters (EDPs) is systematically examined based on 3D computer models of single-story systems by varying their vibration period and response modification factor *R*. This parametric study provides important findings on the significance of rotating ground motions to FN/FP direction and MD. This study further validates these findings by examining both linear and nonlinear responses of multi-story buildings modeled in 3D. The selected systems are 9-story building structures having symmetric and asymmetric lay outs. The computer models are subjected to an ensemble of bi-directional near-fault ground motions with and without distinct velocity-pulses. At the end, this study provides recommendations toward the use of MD and FN/FP direction to rotate ground motion records for RHA of building structures.

POLARIZATON OF VELOCITY-PULSES WITH FAULT-NORMAL/FAULT-PARALLEL AND MAXIMUM-DIRECTIONS

For this investigation, 30 near-fault strong-motion records, listed in Table 1 of the companion paper, were selected from nine shallow crustal earthquakes compatible with a specific scenario. These records were initially rotated to fault-normal (FN) and fault-parallel (FP) orientations, then rotated every 5° in the clockwise direction. Also computed are the velocity-pulse content of the rotated ground motions at each rotation angle θ_x as described in Reyes and Kalkan (2012a). Figure 1 shows the polar plot of identified velocity-pulse periods and spectral accelerations as a function of θ_x for the first 15 records (similar plots for the remaining 15 records are shown in Reyes and Kalkan (2012b)). In these plots, the red dots indicate (i) pulse-periods scaled in polar coordinates and (ii) the directions in which the velocity-pulses are identified. The filled gray area shows ranges of θ_x with velocity-pulses. The dashed blue lines show spectral accelerations computed for a single-degree-of-freedom (SDF) system with T_n equal to the maximum pulse-period of the ground motion (GM) pair at a 5% damping ratio (for example, dashed blue lines for GM1 correspond to spectral accelerations computed for SDF system with T_n = 4.9 sec). The light blue line identifies the maximum-direction angle θ_m. The numerical values for maximum pulse-periods and maximum spectral accelerations are presented in the upper right corner of each sub-plot. An empty polar plot indicates that no velocity-pulse is identified for a given ground motion pair. This figure presents important findings. First, let us examine the GM1 (left upper corner in Figure 1). This polar plot indicates that rotated ground motions have a maximum pulse-period of 4.9 sec. The distinct velocity-pulse is identified for θ_x in between 40°-80° and 130°-170°, and the pulse disappears at other angles including 90° (fault-normal direction). For this record, the maximum-direction angle θ_m is computed at 45° and 135°, in which the velocity-pulse is also identified. Lastly, a maximum spectral acceleration of 0.2 g is observed at θ_m. In the FN-direction, the maximum spectral acceleration is decreased by 30%. Examinations of polar plots of all records permit the following observations:

(1) The velocity-pulses are identified for only 75% of the records. One third of the records with velocity-pulses identified at some rotation angles have no pulses in the FN direction, indicating that the FN-direction doesn't always have a distinct velocity-pulse.

(2) For almost all ground motion pairs, the maximum-direction angle θ_m is in the direction that the velocity-pulse is identified. This strong correlation shows that the maximum spectral acceleration almost always occurs in the direction at which the velocity-pulse is observed.

(3) FN-direction and maximum-direction angle θ_m coincide (within ±5°) for 40% of the records having velocity-pulses, indicating that 60% of the time, maximum spectral acceleration takes place in directions other than the FN-direction.

(4) For a given ground motion pair, the rotation angle θ_x may alter the maximum pulse-period significantly (for example GM6), showing that the pulse-period of rotated components varies with θ_x.

MULTI-STORY STRUCTURES AND COMPUTER MODELS

The structures considered are 9-story symmetric- and asymmetric-plan buildings. The symmetric-plan structure is an existing 9-story steel building with ductile frames (Figure 2a) designed as an office building in southern California according to 2001 California Building Code (ICBO, 2001) for seismic zone 4 and NEHRP soil profile D. The earthquake forces were determined by linear response spectrum analysis for the code design spectrum reduced by a response modification factor of 8.5. The lateral load resisting system consists of two ductile steel moment frames in the longitudinal and transverse directions.

The asymmetric building selected (Figure 2b) is a hypothetical steel building with ductile frames designed to be located in Bell, CA (33.996N, 118.162 W) according to the 1985 Uniform Building Code, which allows for significant plan-irregularity.

Both buildings are modeled for dynamic analysis by the PERFORM-3D computer program (CSI, 2006). The 3D model of the symmetric building has the following features (Reyes and Chopra, 2012): (1) The beams and columns are modeled by a linear element with tri-linear plastic hinges at the ends of the elements. The bending stiffness of the beams is modified to include the effect of the slab. Axial load-moment interactions in columns are based on plasticity theory; (2) Panel zones are modeled as four rigid links hinged at the corners with a rotational spring that represents the strength and stiffness of the connection (Krawinkler, 1978); (3) The tab connections are modeled using rigid perfectly-plastic hinges; (4) The contribution of non-structural elements is modeled by adding four shear columns located close to the perimeter of the building with their properties obtained from simplified models of the façade and partitions. Nonlinear behavior of these elements is represented using rigid-plastic shear hinges; (5) Ductility capacities of girders, columns and panel zones are specified according to the ASCE/SEI 41-06 standard (ASCE, 2007); (6) Columns of moment resisting frames and the gravity columns are assumed to be clamped at the base; and (7) A standard P-Δ formulation is used to approximate effects of nonlinear geometry at large deformations for both moment and gravity frames.

The building was instrumented by fifteen accelerometers. The 2008 magnitude (M_w) 5.4 Chino-Hills earthquake—centered at a distance of 40 km—did not cause any observable damage, and reliable data was recorded. The acceleration records indicate that the peak acceleration of 0.026 g at the ground was amplified to 0.042 g at the roof of the building. This data was used to compute vibration properties of the building by applying two system-identification methods—deterministic-stochastic-subspace (DSS) method (Van Overshee and De Morre, 1996) and the peak-picking (PP) method. As shown in Reyes and Chopra (2012), there is a remarkably close agreement between the calculated (from the computer model) and identified values of vibration periods and modes from the recorded motions.

The beams, columns, panel zones, and P-Δ effects of the asymmetric building were modeled as explained previously for the symmetric-plan building, but the gravity columns were considered pinned at the base. In this system, the period of the dominantly-torsional modes are longer than that of the dominantly-lateral modes (Reyes and Kalkan, 2012b). Also, the higher-mode contributions to forces were expected to be significant because the effective mass of the first lateral mode is less than 50% of the total mass. Details of both buildings and their computer models including model calibration, mode shape plots, effective modal mass values are reported in Reyes and Kalkan (2012b).

EVALUATION METHODOLOGY

The following steps were implemented for evaluating the significance of the ground motion rotation angle on nonlinear behavior of buildings in near fault sites:

(1) For each of the 30 records selected for this investigation, calculate the rotated ground motion components by varying θ_x from 0° to 360° every 10° in the clockwise direction. The motions for θ_x=0° and 90° correspond to the FP and FN components of the record, respectively. In addition, calculate the rotated ground motion components for $\theta_x=\theta_m$ and $\theta_x=\theta_m+90°$. For computing θ_m (maximum direction), use fundamental periods of the buildings.

(2) Conduct linear and nonlinear RHAs of the two building models subjected to bi-directional rotated components of ground motions obtained in Step 1. For each RHA, obtain floor displacements, floor total accelerations, member chord rotations, and beam and column moments. This Step involves 2,400 RHAs.

RESULTS

Linear and nonlinear RHAs were implemented for the 9-story symmetric- and asymmetric-plan buildings subjected to bi-directional excitations following the aforementioned evaluation procedure. Response quantities (EDPs) computed are the story drifts, floor total accelerations, member chord rotations, and beam and column moments at the 1st, 3rd, 5th, 7th, and 9th floors of the buildings. Figure 3 plots the selected EDPs for the linear 9-story symmetric-plan building (T_1 = 1.51 sec) as a function of the rotation angle θ_x subjected to ground motion No. 9, which has a maximum velocity-pulse-period of 1.9 sec. The filled gray area shows the values of θ_x in which the velocity-pulses are identified. The angles θ_x = 0° and 90° correspond to the fault-parallel and fault-normal directions, respectively. The record with a pulse-period close to the fundamental period of the building is selected because such records impose sudden and intense energy input associated with the velocity-pulse that should be dissipated within a short period of time, which causes an amplified deformation demands in structures (Kalkan and Kunnath, 2006, 2007). Figure 3 indicates that maximum values of EDPs generally take place in the same direction, different than the FN-direction, with the exception of the 9th floor *x*-column moment. Also, the maximum EDPs are observed in the direction in which the velocity-pulse is identified. For this particular record, the FN-direction does not contain a distinct velocity-pulse, and the EDPs in the FN-direction are 20% less than their maxima. Same response quantities are plotted in Figure 4 for the linear 9-story asymmetric-plan building (T_1 = 2.5 sec) subjected to ground motion No. 2, which has a velocity-pulse-period of 2.4 sec. It is evident that θ_{cr} varies significantly with EDPs, and there is no optimum angle that leads to the peak values for all EDPs simultaneously.

For a given response quantity of interest and record pair, the FN/FP direction will correspond to two values. By comparing these two values with the responses at all other possible rotation angles, one can evaluate the level of conservatism in such directions; for example whether the FN/FP direction or MD rotated ground motions provide an envelope of an EDP. If obvious systematic benefits of the MD or FN/FP orientations existed, they should be observable by repeating such comparisons for several EDPs and record pairs. To do this, Figure 5 shows the height-wise distribution of the median and dispersion values of story drift plotted separately in *x* and *y* directions for linear-elastic response of the two buildings. In these plots, grey lines represent GMs rotated in 10° increments. The continuous red line is for the FN-direction, and the dashed red line is for the FP-direction. The blue line represents the ground motion components oriented to the MD. Note that each line corresponds to either the median or dispersion of RHA results of 30 ground motion pairs rotated by θ_x.

These figures present important findings. For the linear symmetric-plan system (left panels in Figure 5), the ground motions rotated to FN-direction yield the largest median EDPs in the *x*-direction, whereas in the *y*-direction, the motions oriented in the FP-direction yield the largest median EDPs. Thus, EDPs due to the FN/FP direction rotated ground motions serve as envelopes for all other non-redundant rotation angles. Note that the *x*-direction (longitudinal-direction of the building) coincides with 0° (FP-direction). As opposed to the linear-elastic results based on single-story systems given in the companion paper (Reyes and Kalkan, 2012a), ground motions rotated to MD produce smaller median EDPs as compared to those due to FN/FP direction rotated records. Dispersions of EDPs are also larger in the FN/FP directions than in the MD. For the linear asymmetric system (right panels in Figure 5), neither the FN/FP direction nor the MD rotated ground motion produce the maximum median drift in the *x*-direction. In the same direction, arbitrary orientations resulted in maximum median values. However, in the *y*-direction ground motions rotated to FN/FP direction led to the maximum median drift and floor acceleration. More importantly, the maximum median values of story drift in the *x* and *y* axes corresponded to the MD were smaller than those for the FN/FP direction, indicating that the ground motions rotated to the MD do not necessarily provide unrealistic EDPs as opposed to the critics in Stewart et al. (2011).

Figure 6 shows height-wise distribution of the median+σ[1] and dispersion values of story drift values plotted separately in the *x* and *y* directions for the nonlinear-inelastic responses of the two buildings. In this case, the ground motions rotated to the MD result in the maximum EDPs in the *x*-direction, whereas the same records surprisingly produce the minimum EDPs in the *y*-direction, in which the ground motions oriented to FP-direction yield the largest EDPs. Ground motions rotated to FN-direction produce the second largest EDPs following the results associated with the MD. Therefore, for nonlinear-inelastic response, the MD and FP-direction rotated ground motions serve as envelopes for all other non-redundant rotation angles. This observation is consistent for all EDPs investigated for both symmetric- and asymmetric-plan buildings as shown in Reyes and Kalkan (2012b).

The nonlinear results plotted in Figure 6 (right panels) for story-drift and other EDPs shown in Reyes and Kalkan (2012b) are consolidated and depicted as a function of rotation angle θ_x in Figure 7 and Figure 8 for *x* and *y* axes of the asymmetric-plan building, respectively. Viewing the response as a function of the rotation angle enables us to better understand how the critical angle θ_{cr}, defined as the angle corresponding to the largest response over all angles, changes with both EDP and ground motion pair. It is evident that θ_{cr} leading to the maximum response vary significantly with EDPs. While the FN/FP direction rotated ground motions yield the largest value for certain EDPs, there is no single θ_{cr} that lead to the peak values for all EDPs. Note that the same conclusion was drawn for linear-

[1] 84^{th} percentile of EDPs are plotted to show significant nonlinear response

elastic systems. These two figures prove that the maximum median EDPs (solid red line) are dependent on the rotation angle of the ground motion only for certain EDPs—for example member forces and plastic rotations are not affected by the rotation angle as much as drifts do. The maximum median EDPs due to the MD rotated ground motions yield conservative (either peak or close to peak) results only for the *x*-direction of the building (Figure 7), whereas in the other direction, ground motions oriented to FP-direction provide the most conservative results (Figure 8). Thus, no consistency in over-conservatism of MD rotated ground motions is observed. Results for the symmetric-plan building are similar, therefore not repeated herein but available in Reyes and Kalkan (2012b).

CONCLUSIONS

The influence of the rotation angle of the ground motion on several engineering demand parameters (EDPs) is systematically examined within a parametric study in the companion paper based on three-dimensional (3D) computer models of single-story systems by varying their vibration period and response modification factor *R*. Further validations are performed here using 3D nonlinear computer models of 9-story buildings having symmetric (torsionally-stiff) and asymmetric (torsionally flexible) layouts subjected to a suite of bi-directional near-fault ground motions with and without distinct velocity-pulses. This investigation has led to the following conclusions:

- Velocity-pulses in near-fault records may appear in directions different than the maximum-direction (MD) or fault-normal and fault-parallel (FN/FP) directions. For the near-fault records examined, MD shows large scattering with no visible correlation with the FN/FP directions. This observation is valid even for motions recorded within 5 km of the fault.
- For a given record, the rotation angle leading to the maximum linear-elastic response is different than that leading to the maximum nonlinear-inelastic response; therefore, there is no single rotation angle that operates effectively in both linear and nonlinear domains.
- The maximum drift over all non-redundant orientations seems to be polarized in the direction in which a distinct velocity-pulse with period close to T_1 is observed—this polarization is almost perfect for linear symmetric-plan building.
- Similar to the single-story systems, multi-story structures also show that there is no optimum orientation for a given structure maximizing all EDPs simultaneously. The

maximum value of EDP can happen in any direction different than the direction of the velocity-pulse.

- Conducting nonlinear RHA for ground motions oriented in the FN/FP or maximum-direction does not always lead to the maximum EDPs overall orientations for systems responding in nonlinear-inelastic range. If only few ground motions are used, an underestimation of the peak response may be up to 20%. This observation is true for both symmetric- and asymmetric-plan buildings.
- The ground motions rotated to FN/FP or MD tend to produce larger EDPs than as-recorded (arbitrarily oriented) motions.

Although these observations and findings are primarily applicable to buildings and ground motions with characteristics similar to those utilized in this study, they are in close agreement with the results reported in Kalkan and Kwong (2012a,b), where the influence of the rotation angle on several EDPs has been examined using different structural systems and ground motion records.

ACKNOWLEDGEMENTS

Special thanks are due to Katsuichiro Goda for his critical review on the material presented herein, and offering valuable comments and suggestions, which helped in improving the technical quality of this paper.

REFERENCES

American Society of Civil Engineers, 2010. *Minimum Design Loads for Buildings and Other Structures, ASCE/SEI 7-10*, Reston, VA.

American Society of Civil Engineers, 2006. *Minimum Design Loads for Buildings and Other Structures, ASCE Standard 7-05*, Reston, VA..

American Society of Civil Engineers, 2007. *Seismic Rehabilitation of Existing Buildings, Report No. 41–6*, Reston, VA.

Computers and Structures (CSI), Inc., 2006. *PERFORM 3D, User Guide v4, Nonlinear Analysis and Performance Assessment for 3D Structures*, Computers and Structures, Inc., Berkeley, CA.

International Conference of Building Officials (ICBO), 2009. *International Building Code* Whittier, CA.

International Conference of Building Officials (ICBO), 2010. *California Building Code*, Whittier, CA.

Huang, Y., Whittaker, A. S. and Luco, N., 2008. Maximum spectral demands in the near-fault region, *Earthquake Spectra* **24**(1), 319–34.

Kalkan, E. and Kunnath, S. K., 2006. Effects of fling-step and forward directivity on the seismic response of buildings, *Earthquake Spectra* **22**(2), 367–390.

Kalkan, E. and Kunnath, S. K., 2007. Effective cyclic energy as a measure of seismic demand, *Journal of Earthquake Engineering* **11**(5), 725–751.

Kalkan, E. and Kwong, N. S., 2012a. *Evaluation of Fault-normal/Fault-parallel Directions Rotated Ground motions for Response History Analysis of An Instrumented Six-story Building: U.S. Geological Survey Open-File Report 2012–1058*, available at http://pubs.usgs.gov/of/2012/1058/.

Kalkan, E. and Kwong, N. S., 2012b. Pros and cons of rotating ground motion records to fault-normal/parallel directions for response history analysis of buildings, *ASCE Journal of Structural Engineering* (in-press).

Krawinkler, H., 1978. Shear in beam-column joints in seismic design of frames, *Engineering Journal* **15**(3), 82–91.

Reyes, J. C. and Chopra, A. K., 2012. Modal pushover-based scaling of two components of ground motion records for nonlinear RHA of structures, *Earthquake Spectra* (in press).

Reyes, J. C. and Kalkan, E., 2012a. Significance of rotating ground motions on behavior of symmetric- and asymmetric-plan structures: part 1. parametric study, *Earthquake Spectra* (submitted for publication).

Reyes, J. C. and Kalkan, E., 2012b. *Should Ground motion Records be Rotated to Fault-Normal/Parallel or Maximum-direction for Response History Analysis of Buildings, U.S. Geological Survey Open-File Report 2012*.

Stewart, J. P., Abrahamson, N. A., Atkinson, G. M., Baker, J., Boore, D. M., Bozorgnia, Y., Campbell, K. W., Comartin, C. D., Idriss, I. M., Lew, M., Mehrain, M., Moehle, J. P., Naeim, F., and Sabol, T. A., 2011. Representation of bi-directional ground motions for design spectra in building codes. *Earthquake Spectra* **27**(3), 927–937.

Van Overschee, P. and De Moor, B., 1996. *Subspace Identification for Linear Systems*. Kluwer Academic Publishers, Dordrecht, Boston, London.

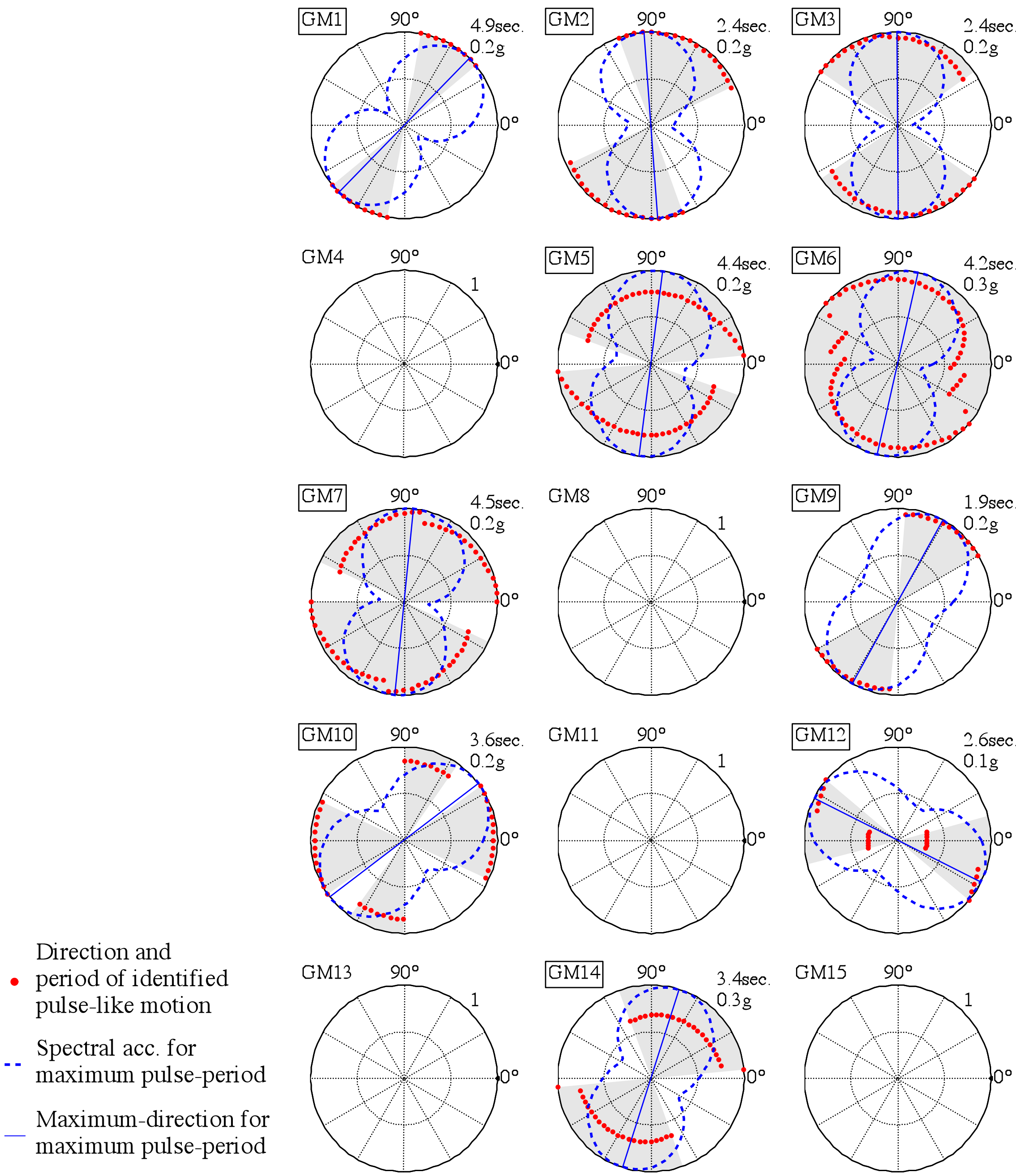

Figure 1. Polar plots of identified velocity-pulse periods and spectral accelerations (damping ratio 5%) as a function of the rotation angle θ_x for ground motion (GM) pairs 1 to 15 (see Table 1 in Reyes and Kalkan (2012a) for a list of GMs). The red dots show the directions in which velocity-pulses are identified with their corresponding pulse-periods. The filled gray area shows range of θ_x with velocity-pulses. The dashed blue lines show spectral acceleration values for the maximum identified pulse-period. The blue solid line identifies the maximum-direction. Numerical values for maximum pulse-periods and maximum spectral accelerations are presented in the upper right corner of each sub-plot. Empty polar plot indicates that no velocity-pulse is identified.

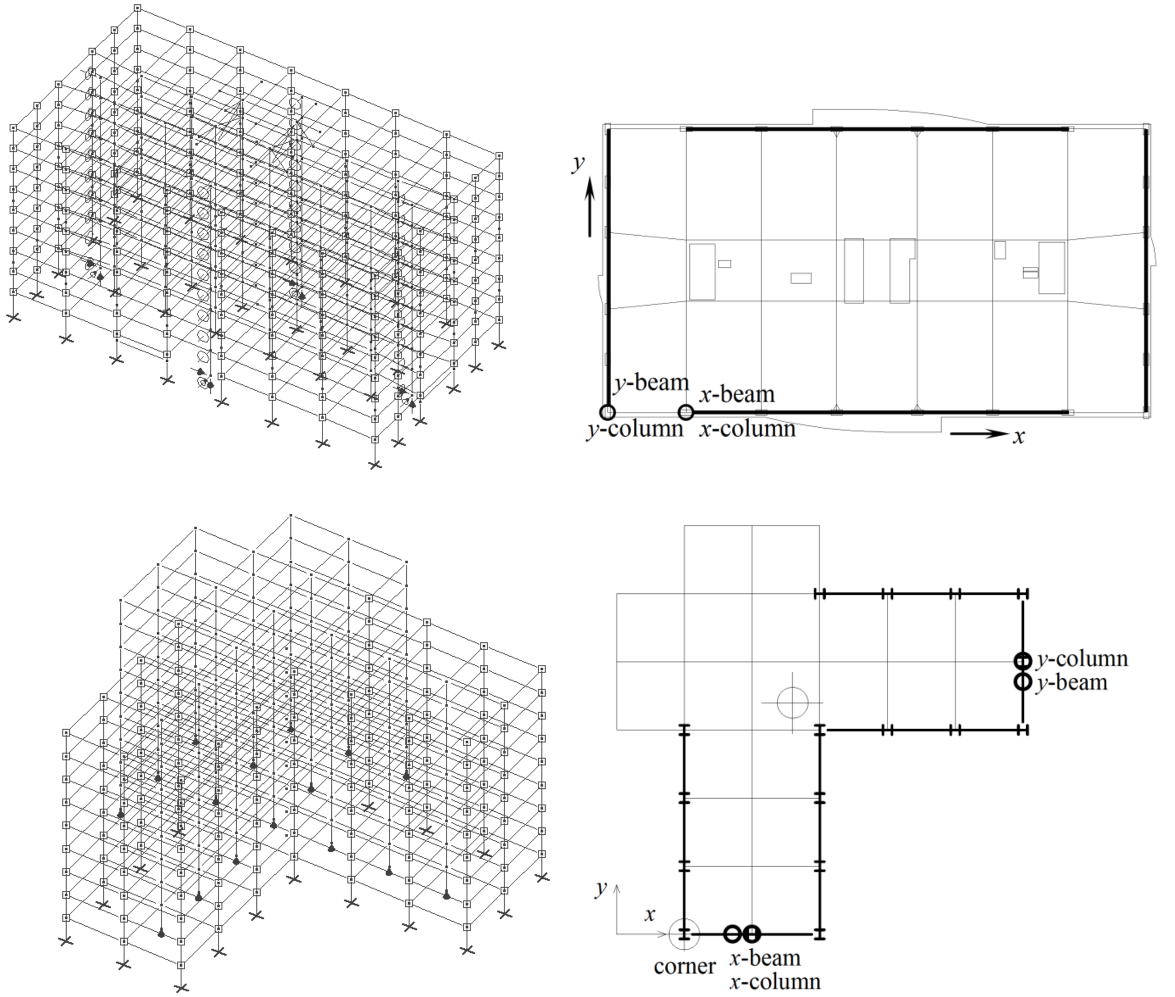

Figure 2. (Top) Nine-story symmetric-plan building; (Bottom) nine-story asymmetric-plan building

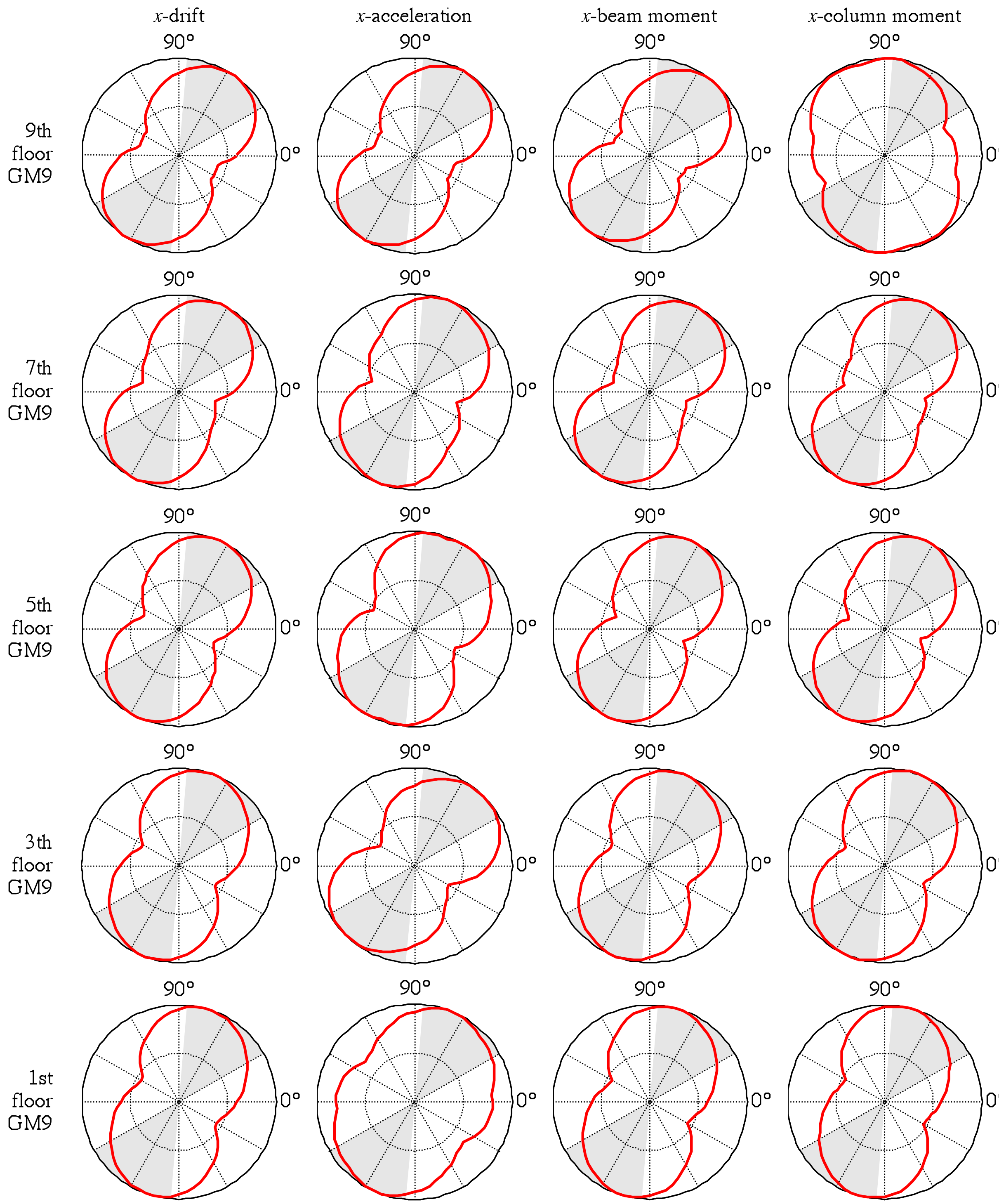

Figure 3. Story drifts, floor total accelerations, and internal forces as a function of the rotation angle θ_x for the linear 9-story symmetric-plan building (T_1 = 1.51 sec) subjected to ground motion (GM) No. 9, which has a maximum velocity-pulse-period of 1.9 sec. The filled gray area shows values of θ_x in which velocity-pulses are identified. Angles $\theta_x = 0^o$ and 90^o correspond to the fault-parallel and fault-normal directions, respectively.

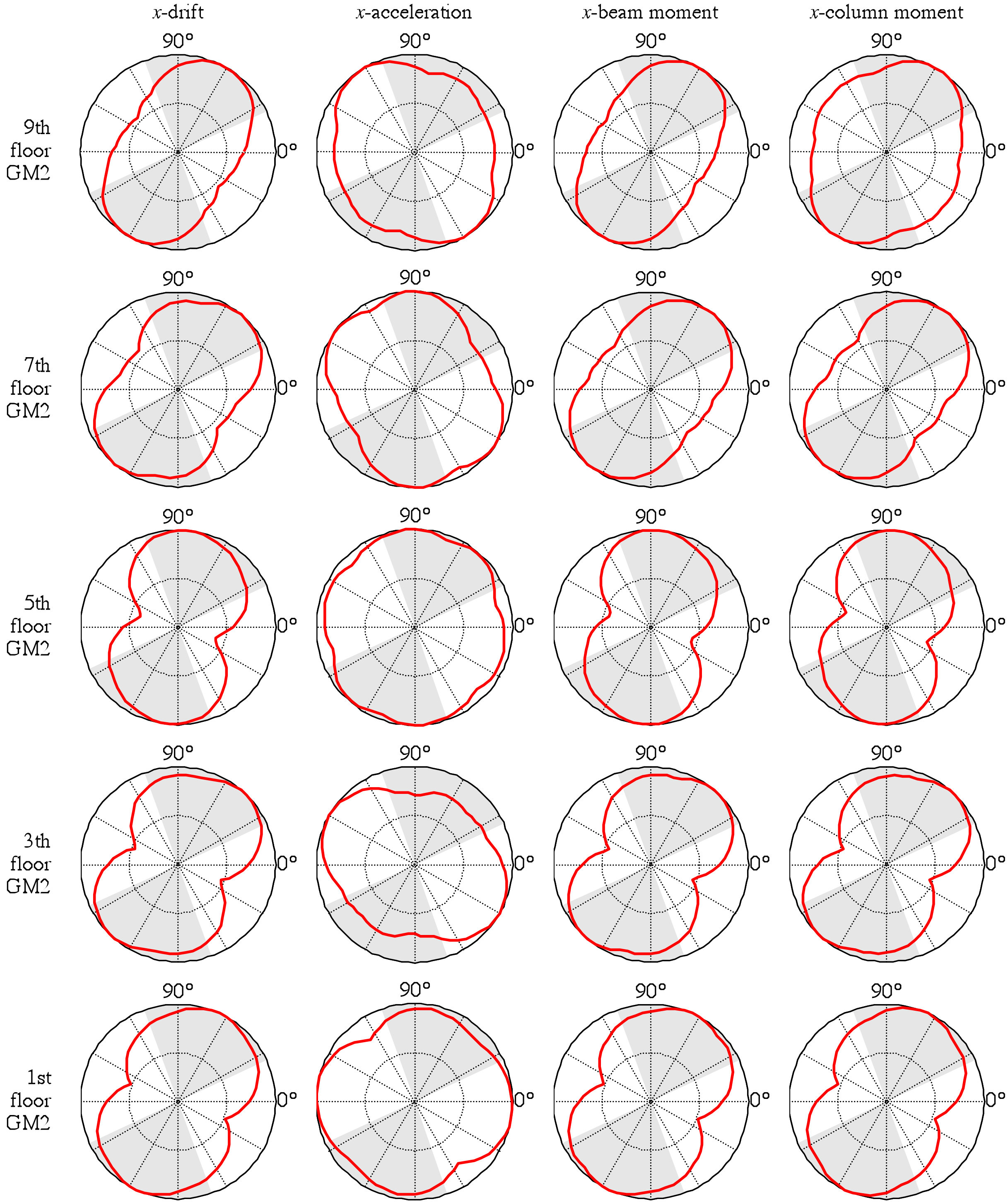

Figure 4. Story drifts, floor total accelerations, and internal forces as a function of the rotation angle θ_x for the linear 9-story asymmetric-plan building (T_1=2.5 sec) subjected to ground motion No. 2, which has a maximum velocity-pulse-period of 2.4 sec. The filled gray area shows values of θ_x in which velocity-pulses are identified. Angles $\theta_x = 0^o$ and 90^o correspond to the fault-parallel and fault-normal directions, respectively.

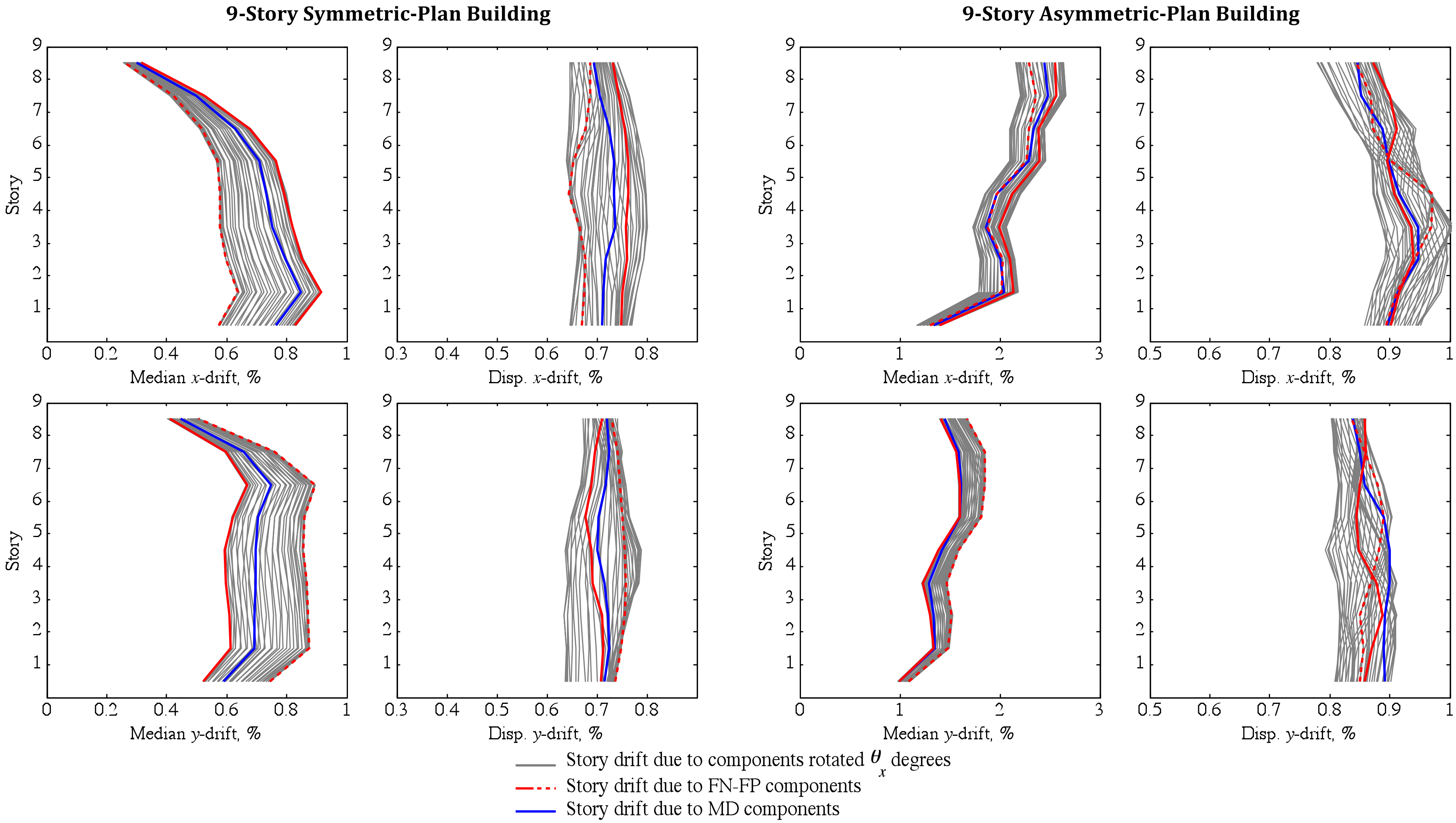

Figure 5. Height-wise distribution of median and dispersion values of story drift in the *x* and *y* directions for the linear 9-story symmetric- and asymmetric-plan buildings. The gray, red, and blue lines show median and dispersion of story drift due to bi-directional ground motions in arbitrary orientations, in the FN/FP directions, and in the maximum-direction, respectively.

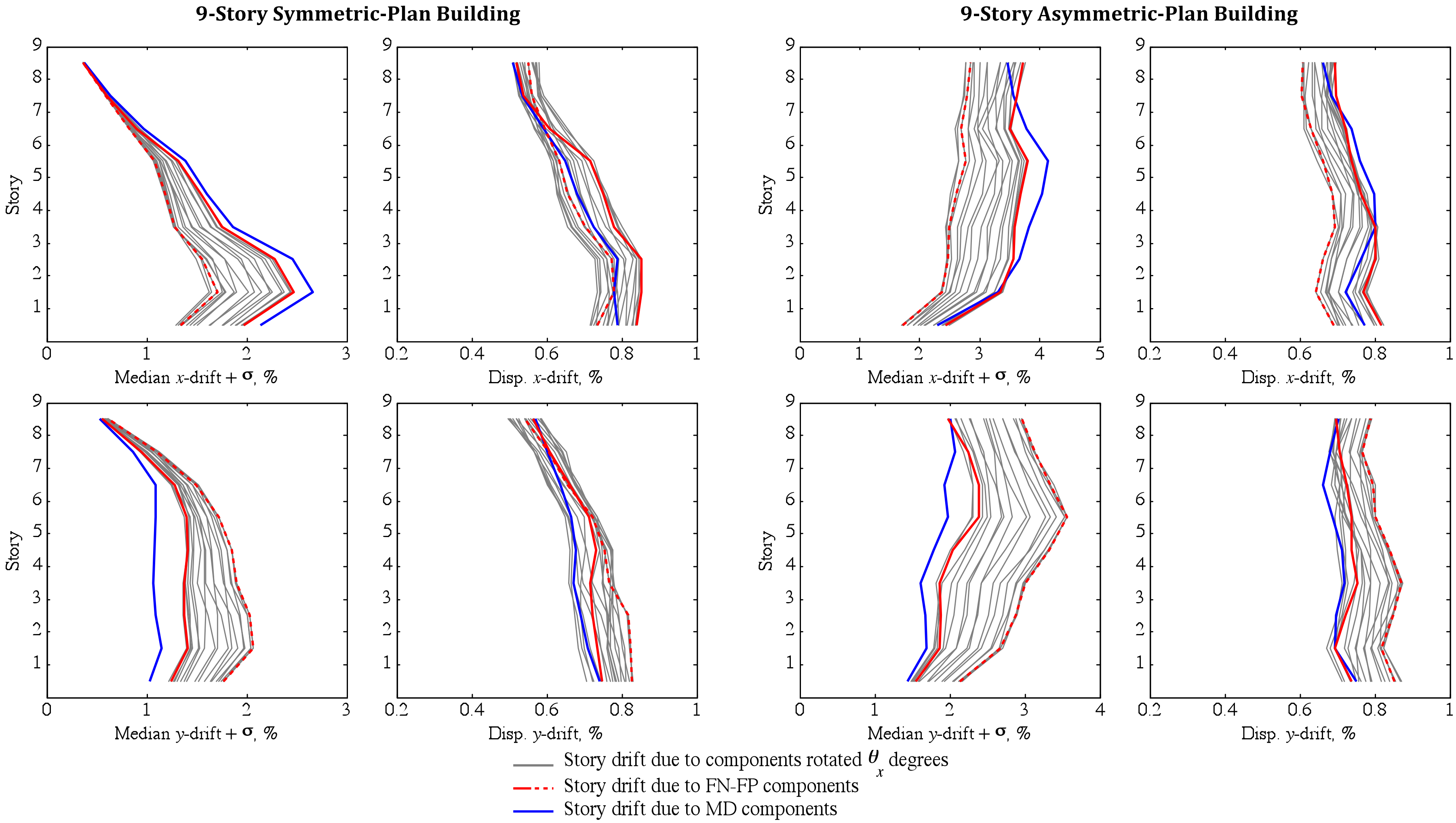

Figure 6. Height-wise distribution of median+σ and dispersion values of story drift in the *x* and *y* directions for the nonlinear 9-story symmetric- and asymmetric-plan buildings. The gray, red, and blue lines show median+σ and dispersion of story drift due to bi-directional ground motions in arbitrary orientations, in the FN/FP directions, and in the maximum-direction, respectively.

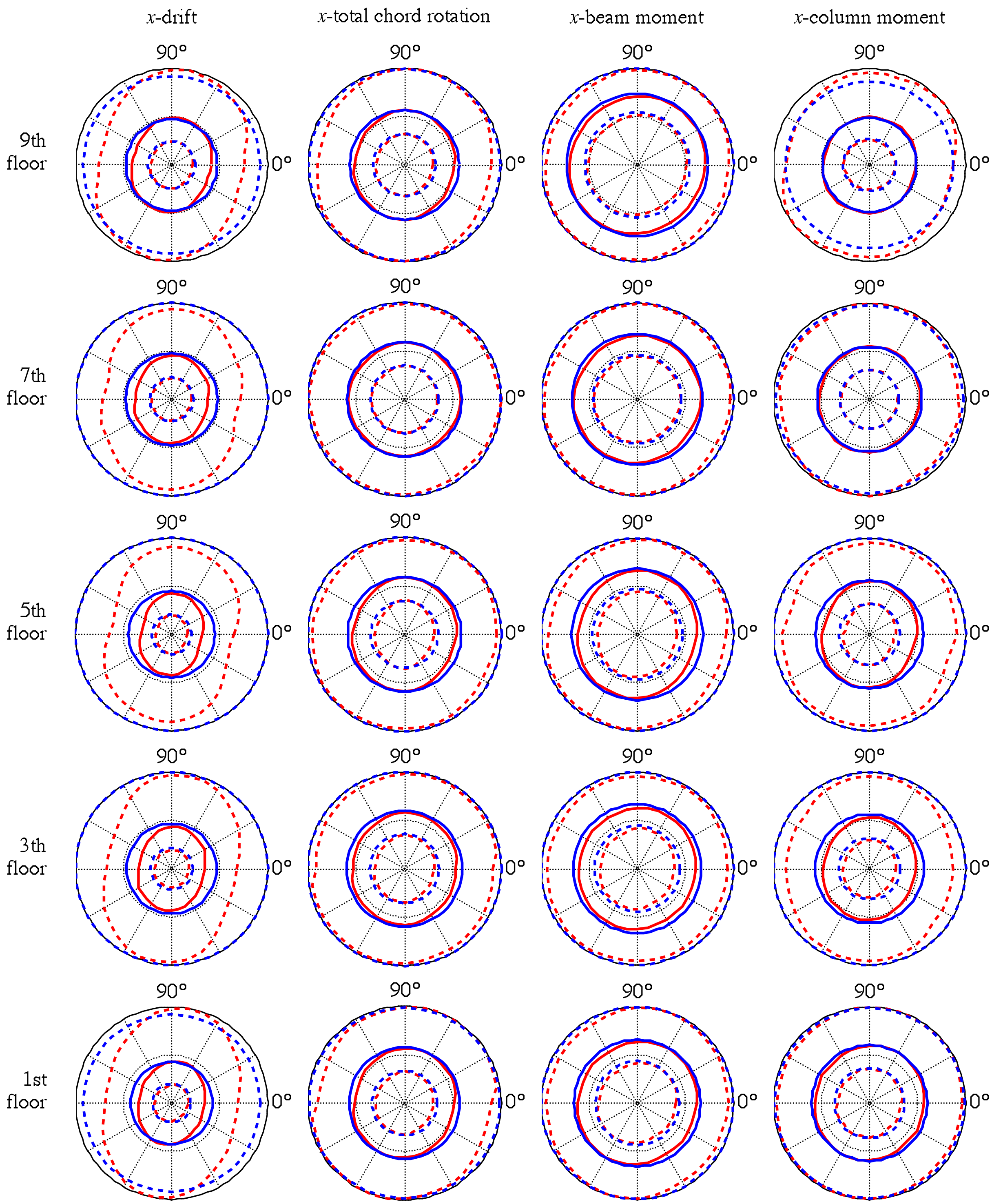

Figure 7. Median values of story drifts at the corner, total chord rotations, and internal forces in the *x*-direction as a function of the rotation angle θ_x for the nonlinear 9-story asymmetric-plan building subjected to bi-directional loading. The red lines represent the median EDP values ± σ. The blue circles represent the median-EDP values ± σ for the building subjected to bi-directional ground motions in the maximum–direction. Note: Median EDP values are shown by solid lines, and 16th and 84th percentile EDP values are shown by dashed lines.

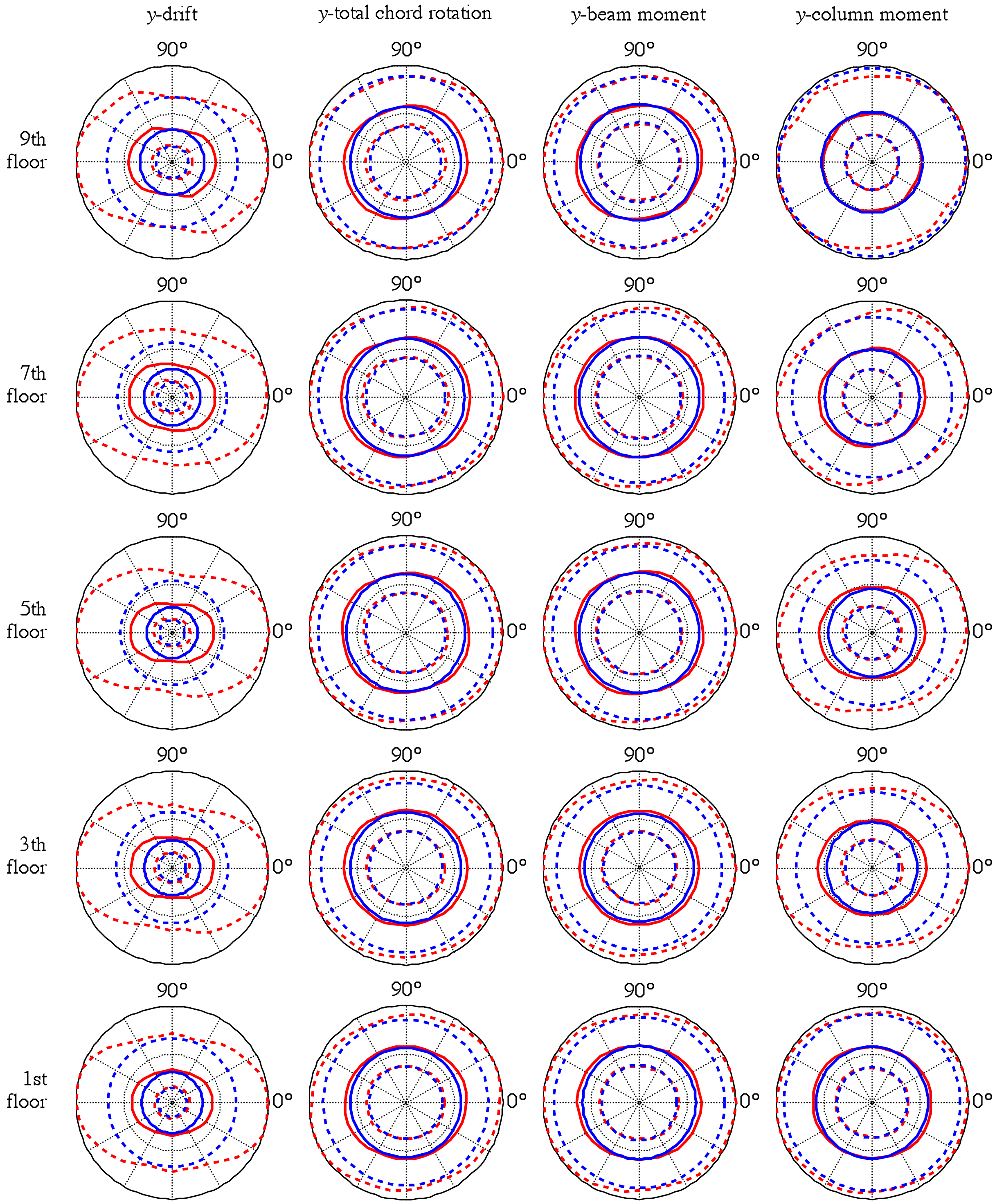

Figure 8. Median values of story drifts, total chord rotations, and internal forces in the y-direction as a function of the rotation angle θ_x for the nonlinear 9-story asymmetric-plan building subjected to bi-directional loading. The red lines represent the median EDP values ± σ. The blue circles represent the median EDP values ± σ for the building subjected to bi-directional ground motions in the maximum–direction. Note: Median EDP values are shown by solid lines, and 16th and 84th percentile EDP values are shown by dashed lines.